PII: S0032-3861(96)00824-5

Polymer Vol. 38 No. 11, pp. 2711–2718, 1997

0032-3861/97/$17.00 + 0.00

Crystallization of ε-caprolactone blocks within a crosslinked microdomain structure of poly(ε-caprolactone)-*block*-polybutadiene

Shuichi Nojima*, Ken Hashizume, Awaludin Rohadi and Shintaro Sasaki
School of Materials Science, Japan Advanced Institute of Science and Technology (JAIST), Tatsunokuchi, Ishikawa 923-12, Japan
(Received 25 July 1996)

The morphology, formed by the crystallization of ε-caprolactone blocks in a crosslinked microdomain structure of poly(ε-caprolactone)-*block*-polybutadiene (PCL-*b*-PB), has been investigated by wide-angle X-ray diffraction (WAXD), small-angle X-ray scattering (SAXS), and differential scanning calorimetry (d.s.c.). The WAXD results showed that even in the crosslinked PCL-*b*-PB, PCL blocks crystallized in the same crystal form as PCL homopolymers. The SAXS measurements revealed that the microdomain structure in the melt remained unchanged by the subsequent crystallization, indicating that the PCL blocks crystallized within this structure. This point is extremely different from the case of the uncrosslinked PCL-*b*-PB, where a dramatic morphological reorganization takes place by the crystallization; a microdomain structure is completely replaced by an alternating structure of lamellae and amorphous layers. The melting temperature and crystallinity of the PCL blocks in the crosslinked PCL-*b*-PB were significantly reduced compared with those of the uncrosslinked PCL-*b*-PB, suggesting that the fixed microdomain structure affected significantly the crystallization of the PCL blocks to yield imperfect crystals within this structure. © 1997 Elsevier Science Ltd.

(Keywords: crystalline-amorphous diblock copolymer; microdomain structure; crystallization)

INTRODUCTION

The morphology formed in crystalline-amorphous diblock copolymers is complicated by a combined effect of crystallization of the constituent block and microphase separation between different blocks. In recent years, there have been several theoretical and experimental studies on the morphology and morphology formation of such block copolymers[1–15]. In the case of relatively low molecular weight copolymers[3–10], where the temperature of microphase separation is close to the melting temperature of the crystallizable block, the microdomain structure is completely destroyed by the subsequent crystallization, as demonstrated in the systems of poly(ε-caprolactone)-*block*-polybutadienes[4,7] and polyethylene-*block*-poly(ethylethylene)s[8]. This is because the free energy reduction due to the microphase separation is not large enough and the crystallization can easily overcome the free energy barrier necessary to destroy this structure. In the case of high molecular weight copolymers, on the other hand, an extreme reduction in free energy due to the microphase separation leads to freezing of the resultant structure and the crystallization takes place substantially within this structure[11–15]. To examine the crystallization behaviour and final morphology within the microdomain structure, it is a convincing method to fix the structure completely by the chemical crosslinks of the constituent block in order to prevent further reorganization of the microdomain structure.

There are several experimental studies on the crosslinked polymer systems[16–23], where the influence of crosslinks on the crystallization mechanism, final morphology, or miscibility is discussed as compared with the case of uncrosslinked systems. Shibayama *et al.*[22,23], for example, investigated the crystallization behaviour of end-linked poly(tetrahydrofuran)s (PTHF) and showed that PTHF segments restricted in the network could crystallize to result in immature spherulites. This fact suggests that the subsequent morphology formation occurs even within the crosslinked systems although the mode of this morphology formation is significantly altered.

In this study, we try to crystallize the ε-caprolactone blocks within a crosslinked microdomain structure of poly(ε-caprolactone)-*block*-polybutadiene. It is possible to fix the microdomain structure completely by introducing chemical crosslinks to the PB blocks at the molten state. By this method, we can get the crosslinked samples with a definite structure. The final morphology on the subsequent crystallization is examined by WAXD and SAXS, and the melting behaviour is also investigated by d.s.c. The results obtained are compared with those of the uncrosslinked PCL-*b*-PB and we elucidate the influences of the fixed microdomain structure on the crystallization and final morphology.

* To whom correspondence should be addressed

EXPERIMENTAL

Materials

The poly(ε-caprolactone)-*block*-polybutadiene (PCL-*b*-PB) used in this study (denoted B17 in our recent study[9]) was synthesized by successive anionic polymerizations under vacuum with *n*-butyllithium as an initiator. Details of the synthesis were described elsewhere[4,7]. The molecular characteristics of this copolymer are as follows: the number-average molecular weight (M_n) evaluated by vapour pressure osmometry is 18000, the polydispersity index (M_w/M_n) by gel permeation chromatography is 1.38, the PCL content in the copolymer by ^{1}H n.m.r. is 26 vol%, and the microstructure of the PB block by ^{1}H n.m.r. is 34, 49 and 17 mol% for *cis*-1,4, *trans*-1,4, and 1,2-linkage, respectively. This copolymer has a hexagonally-packed cylindrical structure in the melt judging from the PCL content and the angular position of small-angle X-ray intensity peaks (*Figure 7a*)[24].

The poly(ε-caprolactone) homopolymer (PCL), used for comparison purposes of the crystal structure, was supplied from Scientific Polymer Products Inc., and M_n and M_w/M_n were stated to be 10700 and 3.1, respectively.

Method of crosslinks

The microdomain structure in the melt was fixed by a crosslink reaction between the double bond of the PB block and peroxide, 1,1-bis(*tert*-butylperoxy)-3,3,5-trimethylcyclohexane. This peroxide is known to react only with PB blocks at high temperatures (~150°C) to introduce crosslinks in the system[25]. Actually, PCL did not react at all with the peroxide at 150°C.

The peroxide was first dissolved homogeneously with a PCL-*b*-PB/benzene solution, and the benzene solution was subsequently cast on a glass plate to get homogeneous thin films of PCL-*b*-PB and peroxide. The mole number of the peroxide against that of PCL-*b*-PB, *n*, was changed in the range between 0.3 and 3.0 to check the influence of the crosslink density on the final morphology and melting behaviour after crystallization. The film was then annealed at *ca.* 60°C for 30 min to destroy the previous morphology at room temperature and to develop the cylindrical microdomain structure, and followed by the heat treatment at 150°C for 30 min to introduce crosslinks in the PB region, where PCL-*b*-PB still had the cylindrical microdomain structure judging from the SAXS curve at 150°C. Finally the film was washed with benzene several times to remove the uncrosslinked PCL-*b*-PB. The macroscopic degree of PCL-*b*-PB crosslinked by this reaction, *f*, was estimated from a weight ratio of remaining films and initial copolymers. We denote hereafter the un-crosslinked PCL-*b*-PB as PCL-*b*-PB(U) and the crosslinked PCL-*b*-PB as PCL-*b*-PB(C).

WAXD measurements

The WAXD measurement was performed with Rigaku diffractometer (RAXIS 200 IIC) using Ni-filtered CuK_α radiation supplied by a Rigaku RU300 generator operating at 40 kV and 100 mA. The detector was an imaging plate with 512 × 512 pixels. The two-dimensional data were reduced to one-dimensional data through a circular average and then the background and amorphous halo were subtracted from the WAXD pattern to evaluate the characteristic diffractions from the PCL crystal. The samples were about 1 mm in thickness and crystallized at room temperature for 3 days to ensure the complete crystallization.

SAXS measurements

The SAXS measurement was performed with a point focusing optics and a one-dimensional position sensitive proportional counter (PSPC) with an effective length of 10 cm. The SAXS optics has a toroidal mirror and a two-crystal monochromator to focus the scattered intensity on the PSPC. The CuK_α radiation supplied by a MAC Science M18X generator operating at 40 kV and 30 mA was used throughout. The distance between the sample and PSPC was about 40 cm. The geometry was further checked by a chicken tendon collagen, which gives a set of sharp diffractions corresponding to 65.3 nm.

The sample was kept for a long time before measurements at a measuring temperature T_a by circulating temperature-controlled water to the sample holder. The fluctuation of T_a was less than 1°C throughout. When T_a was lower than room temperature, the sample was crystallized at another place and moved to the sample holder. The time necessary for each SAXS measurement was 3000 s.

The SAXS intensity measured was corrected for background scattering and absorption by the sample. The angular position of the intensity peak and the full width at half maximum (FWHM) were evaluated as a function of T_a for PCL-*b*-PB(U) and PCL-*b*-PB(C).

D.s.c. measurements

A Perkin–Elmer Model 7 DSC was used to determine the melting temperature T_m of the PCL block and block crystallinity χ, i.e., wt% of crystallized PCL blocks against existing PCL blocks in the system. The sample, first annealed at 65°C for 1 h, was quenched by a maximum quenching rate (=500°C min^{-1}) to the crystallization temperature T_c ranging from 15°C to 45°C for PCL-*b*-PB(U) and from −20°C to 30°C for PCL-*b*-PB(C), followed by heating at a rate of 3°C min^{-1}. T_m was evaluated from the endothermic peak position and χ was calculated from the peak area assuming that the heat of fusion for the perfect PCL crystal is 135.44 J g^{-1} [26].

RESULTS AND DISCUSSION

Influence of crosslink density on the final morphology

In this study, the concentration of peroxide was changed to examine the influence of the crosslink density on the final morphology after crystallization of the PCL block. We did not, however, try to estimate the actual crosslink density because the difference in this density did not affect the following results at all. The density might affect significantly, for example, the kinetics of crystallization and mechanical properties of the system[23].

The PCL-*b*-PB(C) obtained was macroscopically characterized by the wt% fraction, *f*, of crosslinked specimens against initial copolymers, which is defined by the equation,

$$f(\mathrm{wt\%}) = 100 \times (w/w_0)$$

where w_0 and w are the weights of PCL-*b*-PB before and after the crosslink reaction, respectively. Note that *f* does not represent directly the crosslink density in the system, but it is likely that increasing *n* means the increase of the crosslink density. *Figure 1* shows the *n* dependence of *f*

for PCL-*b*-PB(C), where n denotes the number of peroxide against each PCL-*b*-PB molecule. The value of f is about 60 wt% irrespective of n. Even when the peroxide was absent in the system ($n = 0$ in *Figure 1*), we could obtain the crosslinked gel ($f \sim 40$ wt%) insoluble to benzene only by the heat treatment at 150°C for 30 min, although this gel was more flexible and hence weakly crosslinked compared to PCL-*b*-PB(C).

The n dependences of the melting temperature T_m and block crystallinity χ for PCL-*b*-PB(C) are shown in *Figure 2*. The data on the ordinate correspond to those for PCL-*b*-PB(U). Although T_m and χ for PCL-*b*-PB(C) are significantly lower than the values for PCL-*b*-PB(U), they are independent of n as long as n is in the range between 0.3 and 3.0. This means that the final morphology and melting behaviour described below are not affected by the crosslink density, while they are extremely dependent on whether the crosslinks exist or not in the system. We used PCL-*b*-PB(C) with $n = 1$ for the following WAXD, d.s.c., and SAXS measurements.

WAXD measurements

In order to check the crystallizability and crystal structure of the PCL block in PCL-*b*-PB(C), we examined WAXD patterns of PCL, PCL-*b*-PB(U), and PCL-*b*-PB(C) (*Figure 3*). Each WAXD pattern has a couple of crystallographic reflections, which can be indexed satisfactorily to the crystal structure of PCL[27]. This indicates that the PCL blocks certainly crystallize even in PCL-*b*-PB(C) in the ordinary crystal form. A significant broadening of the reflections, however, cannot be detected among the WAXD patterns shown in *Figure 3* and we cannot extract information about the difference in crystal perfection between PCL-*b*-PB(U) and PCL-*b*-PB(C).

Lovinger *et al.*[6] examined the crystal structure of PCL blocks in PCL–poly(dimethyl siloxane)–PCL triblock copolymers and obtained the diffraction patterns identical to PCL to confirm the presence of PCL crystals in their triblock copolymers. Register *et al.*[5] observed diffraction patterns of polyethylene in a series of polyethylene-*block*-poly(ethylene-*alt*-propylene)s to get the crystallinity of polyethylene blocks. These facts lead us to conclude that the crystal structure of the constituent block in the copolymer is identical with the corresponding homopolymer. In addition, we feel that crystallization is a strong factor to bring about the morphology formation even in the systems where the molecular motion is extremely restricted, as demonstrated in the crystallization of crosslinked polyethylenes[19–21] and end-linked poly(tetrahydrofuran)s[22,23].

D.s.c. measurements

Figure 4a shows the melting curves for PCL-*b*-PB(U) crystallized at each temperature indicated. At $T_c = 42$, 40, and 37°C, the curves are bimodal with both peak temperatures decreasing with decreasing T_c. At $T_c = 35$ and 30°C, on the other hand, there is a single endothermic peak, although a faint shoulder can be detected at $T_c = 35$°C. These melting curves were strongly dependent on the crystallization time t_c at each T_c; the lower temperature peak decreased and the higher temperature peak (and also block crystallinity) increased with increasing t_c.

The multiple melting peaks are sometimes observed in crystalline homopolymers where recrystallization occurs

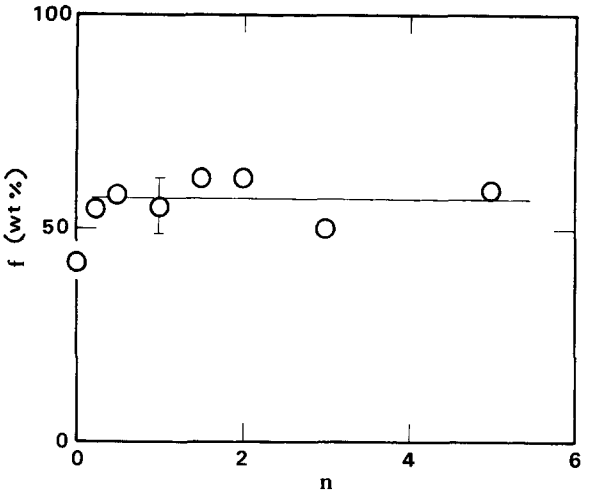

Figure 1 Plot of the wt% fraction of PCL-*b*-PB(C), f, against the concentration of peroxide n. n represents the number of peroxide against each PCL-*b*-PB molecule

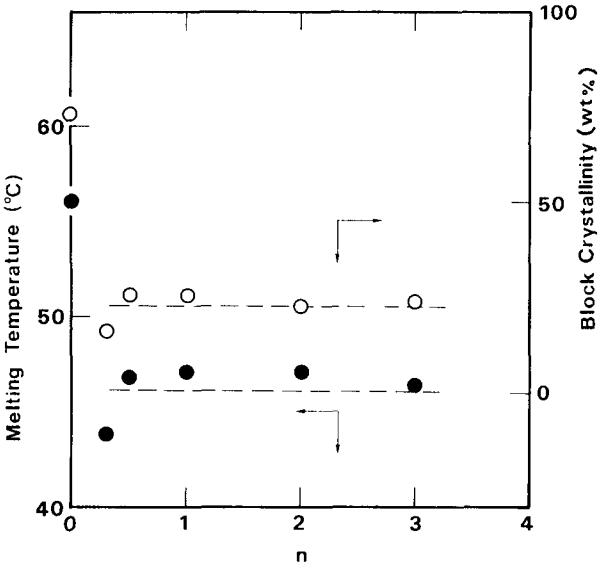

Figure 2 Plots of the melting temperature T_m and block crystallinity χ against n. The symbols on the ordinate correspond to the results of PCL-*b*-PB(U)

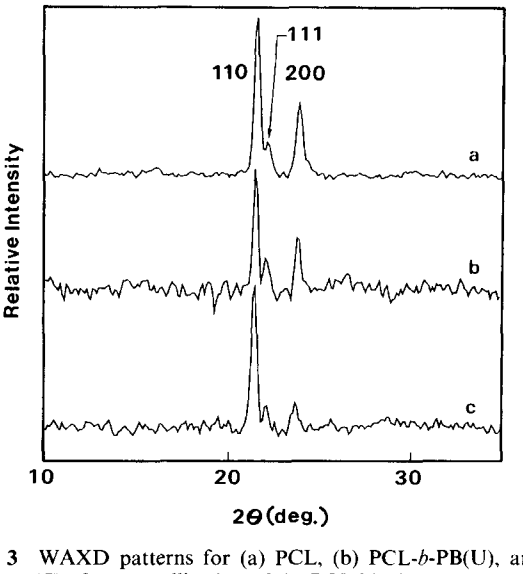

Figure 3 WAXD patterns for (a) PCL, (b) PCL-*b*-PB(U), and (c) PCL-*b*-PB(C) after crystallization of the PCL block

on heating, that is, thinner lamellae melt at a lower temperature to yield thicker lamellae with higher T_m[28]. The bimodal thermogram, therefore, depends significantly on the heating rate. In the present PCL-*b*-PB, there is another possibility to yield such bimodal melting curves, because the PCL homopolymer, identical to the crystallizable block in PCL-*b*-PB, did not show the definite bimodal melting behaviour at any T_c. That is, the system might have two morphologies, microdomain structure and lamellar morphology, at the beginning of crystallization, in which the crystallization mechanism and hence final morphology should be different giving different T_m. If this is the case, this bimodal melting curve is characteristic of the crystallization of block copolymers, as discussed later.

The melting curves for PCL-*b*-PB(C) crystallized at each temperature are shown in *Figure 4b*, where the ordinate is enlarged by a factor of 3 to be compared with *Figure 4a*. The crystallization did not occur substantially in the temperature range where PCL-*b*-PB(U) crystallized, and it was necessary to lower T_c extremely. One endothermic peak was detected at each T_c although it was small and broad compared to that of PCL-*b*-PB(U). *Figure 4* indicates clearly that the introduction of crosslinks in the system changes dramatically the melting behaviour of the PCL block and hence final morphology in the system. Particularly, the low T_m and low crystallinity arise from the decelerated crystallization within the crosslinked morphology.

Melting temperature and crystallinity

The T_c dependence of T_m for PCL-*b*-PB(C) and PCL-*b*-PB(U) is shown in *Figure 5*. The higher T_m for PCL-*b*-PB(U) decreases with decreasing T_c and levels off below $T_c = 37°C$, which is usually observed for the melting behaviour of crystalline homopolymers. The lower T_m, on the other hand, decreases steeply with decreasing T_c and seems to connect smoothly with T_m for PCL-*b*-PB(C). This fact makes us speculate that the lower T_m corresponds to the melting of the PCL blocks crystallized

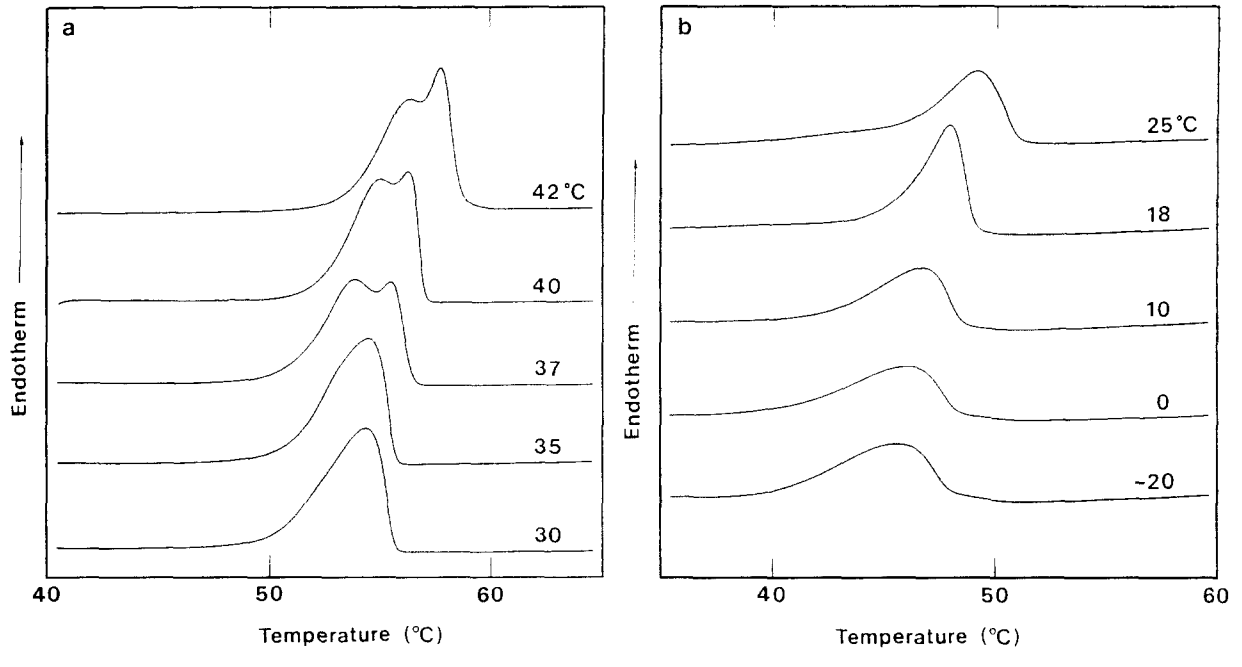

Figure 4 D.s.c. thermograms of (a) PCL-*b*-PB(U) and (b) PCL-*b*-PB(C) crystallized at each temperature indicated. The heating rate is 3°C min^{-1}. The ordinate in (b) is enlarged by a factor of 3 for clarity

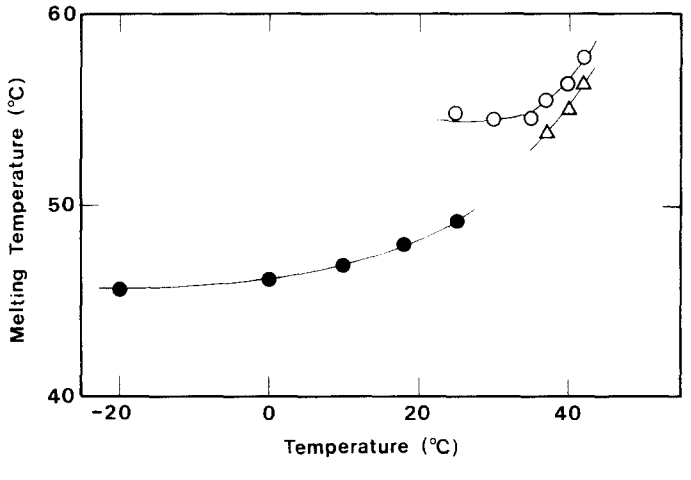

Figure 5 Melting temperature T_m plotted against T_c for PCL-*b*-PB(U) (○, △) and PCL-*b*-PB(C) (●)

within the existing microdomain structure. That is, the PCL blocks crystallize within the microdomain structure (*crystallized microdomain structure*) and simultaneously the morphological reorganization occurs from the microdomain structure into the alternating structure of lamellae and amorphous layers (*lamellar morphology*). The system, therefore, has two morphologies at the beginning of crystallization. The crystallized microdomain structure will show a lower T_m than the lamellar morphology, because the crystallization in the microdomain structure is more restricted to give the imperfect PCL crystals. Detailed analysis of the crystallization and melting behaviours of PCL-*b*-PB(U) will appear in the forthcoming paper[29].

Figure 6 shows the T_c dependence of χ for PCL-*b*-PB(C) and PCL-*b*-PB(U). The value χ for PCL-*b*-PB(C) is *ca.* 1/3 of that for PCL-*b*-PB(U) and is almost constant irrespective of T_c. *Figure 6* also suggests our speculation mentioned above, that is, the PCL crystals within the microdomain structure are immature to yield a large reduction of the block crystallinity. The constant χ against T_c is not usually observed in crystalline homopolymers, suggesting that the sub-morphology on crystallization within the microdomain structure will be specific although a definite picture cannot be presented here.

SAXS measurements

The SAXS intensity curves for PCL-*b*-PB(U) at various temperatures are shown in *Figure 7a*. At 69.5°C ($>T_m$), a cylindrical microdomain structure appears in the system and we can get a set of diffractions (shown by arrows in *Figure 7a*) from this structure. At temperatures below T_m, on the other hand, the PCL blocks crystallize by destroying the existing microdomain structure to result in the formation of lamellar morphology and hence the SAXS curves change dramatically. That is, the angular position of the intensity peak shifts

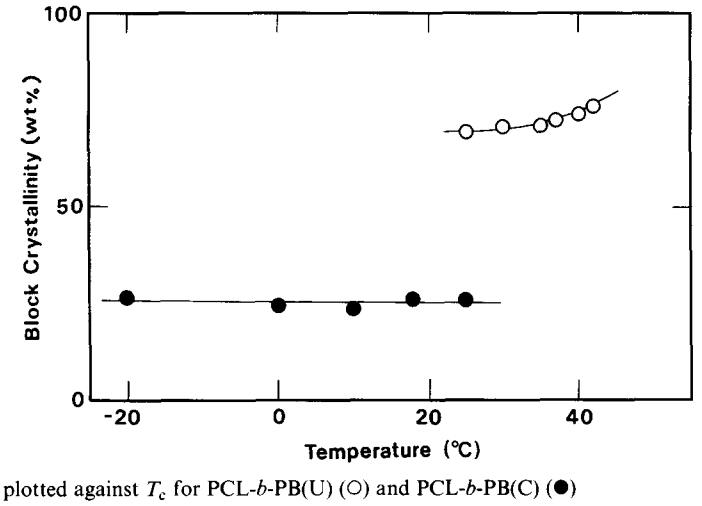

Figure 6 Block crystallinity χ plotted against T_c for PCL-*b*-PB(U) (○) and PCL-*b*-PB(C) (●)

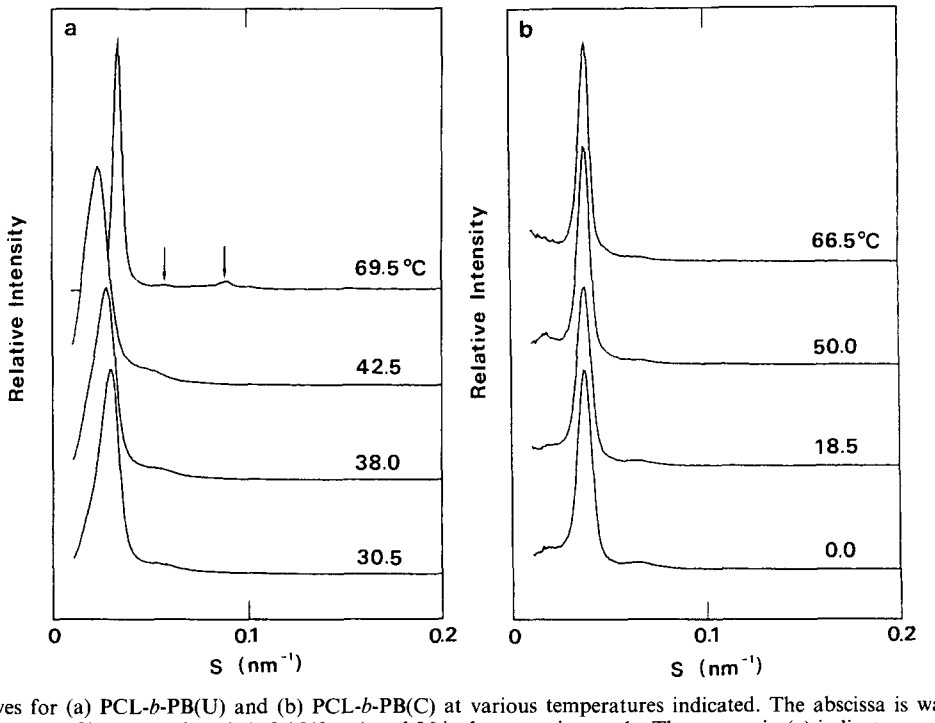

Figure 7 SAXS curves for (a) PCL-*b*-PB(U) and (b) PCL-*b*-PB(C) at various temperatures indicated. The abscissa is wave number defined as $s = (2/\lambda)\sin\theta$, where λ is the X-ray wavelength (=0.1542 nm) and 2θ is the scattering angle. The arrows in (a) indicate second and third scattering peaks

significantly to the lower angle with the peak width being broad. In addition, the peak position is strongly dependent on T_c as previously reported for various PCL-*b*-PB copolymers[4,7,9]. This morphological transition has been confirmed by electron microscopy in our recent study[9].

The SAXS intensity curves for PCL-*b*-PB(C) at various temperatures are shown in *Figure 7b*. From the d.s.c. results, the PCL blocks crystallize at 0°C and 18.5°C, while it is amorphous at 50°C and 66.5°C. The SAXS curves shown in *Figure 7b* are similar in shape irrespective of T_a, which is quite different from the case of PCL-*b*-PB(U) shown in *Figure 7a*. That is, the microdomain structure in PCL-*b*-PB(C) is preserved by the subsequent crystallization. An additional scattering reflecting the inside of the microdomain structure (sub-morphology) is, however, not observed in *Figure 7b*.

Figure 8 shows the T_a dependence of spacings evaluated from the angular position of the intensity peak for PCL-*b*-PB(U) and PCL-*b*-PB(C). As expected from *Figure 7*, the spacing changes dramatically for PCL-*b*-PB(U) at around T_m, while it is almost constant for PCL-*b*-PB(C). This is the most different point in morphology between PCL-*b*-PB(U) and PCL-*b*-PB(C). The spacing of the microdomain structure reduces by *ca.* 10% before and after the crosslink reaction, indicating that the microdomain structure shrinks slightly. This small shrinking in morphology was also reported in the crosslinked polystyrene-*block*-polybutadiene-*block*-polystyrene copolymers[18].

Figure 9 shows the T_a dependence of the full width at half maximum (FWHM) of the intensity peak, Δw, for PCL-*b*-PB(U) and PCL-*b*-PB(C). At above T_m, Δw is identical for both samples. Below T_m, on the other hand, the temperature dependence of Δw is quite different; for PCL-*b*-PB(C), Δw increases slightly, indicating that the microdomain structure existing above T_m distorts slightly by the crystallization to produce the distribution in the regular arrangement of this structure. That is, the crosslinked microdomain structure is not tight enough but transformable depending on the conformation of the constituent blocks. The value of Δw for PCL-*b*-PB(U), on the other hand, increases suddenly at T_m, reflecting

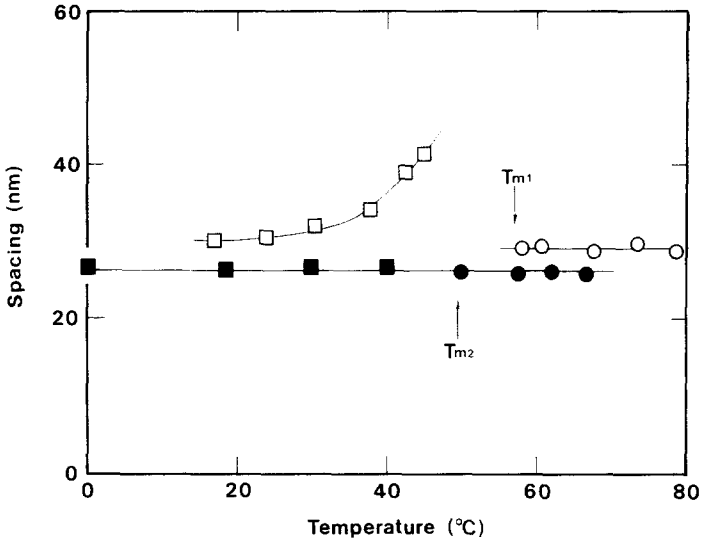

Figure 8 Spacings evaluated from the angular position of the SAXS intensity peak plotted against T_a for PCL-*b*-PB(U) (□, ○) and PCL-*b*-PB(C) (■, ●). T_{m1} and T_{m2} represent the melting temperatures of PCL-*b*-PB(U) and PCL-*b*-PB(C), respectively

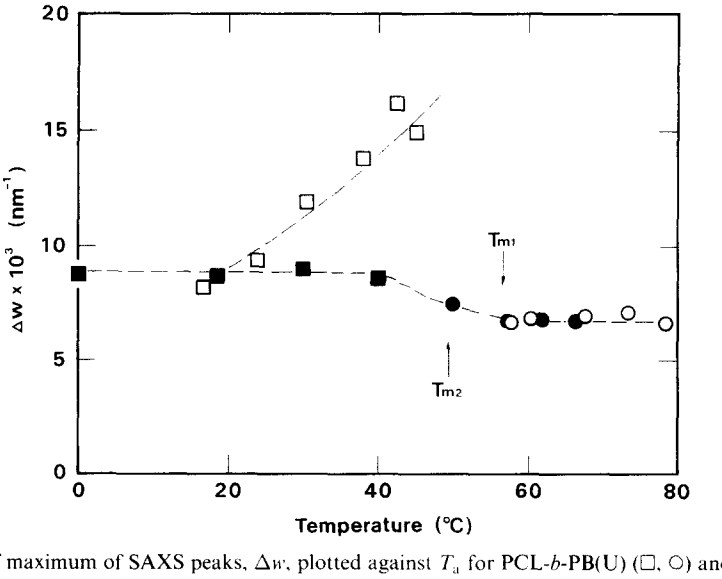

Figure 9 The full width at half maximum of SAXS peaks, Δw, plotted against T_a for PCL-*b*-PB(U) (□, ○) and PCL-*b*-PB(C) (■, ●)

the development of a new lamellar morphology in the system.

Morphological consideration

The results described above clearly show that the PCL blocks in PCL-*b*-PB(C) crystallize within the fixed microdomain structure to yield imperfect crystals with a low T_m and a low χ, which is contrary to the case of PCL-*b*-PB(U), where the crystallization brings about a dramatic change in morphology from the microdomain structure into the lamellar morphology. *Figure 9*, however, shows that the fixed microdomain structure distorts slightly by the subsequent crystallization of the PCL block.

The morphological change on crystallization both for PCL-*b*-PB(U) and PCL-*b*-PB(C) is schematically shown in *Figure 10* on the basis of the present results. In the case of PCL-*b*-PB(U) (*Figure 10a*), the microdomain structure is completely replaced into the lamellar morphology after a long time and details of this morphology (lamellar thickness, amorphous layer thickness, and so on) are determined by a delicate balance of free energies between the amorphous and crystalline blocks, as theoretically predicted by DiMarzio *et al.*[1] and Whitmore and Noolandi[2]. In the case of PCL-*b*-PB(C) (*Figure 10b*), on the other hand, the microdomain structure is substantially frozen and the PCL blocks have to crystallize within this structure. Therefore, the crystallization mechanism and the resultant PCL crystals should be extremely different from the case of PCL-*b*-PB(U).

The crystallization of the PCL blocks will produce the volume contraction of the cylindrical microdomain structure; a 25% block crystallinity (*Figure 6*) corresponds to *ca.* 2.4% contraction of the cylinder volume at 20°C[26,27]. This volume contraction is considered to yield the distortion of the microdomain structure (*Figure 9*). In other words, the volume contraction may restrict the crystallinity of the PCL blocks, because a high crystallinity will produce a large volume contraction and hence a large deformation of the microdomain structure. The crystallization behaviour of PCL-*b*-PB(C) is, therefore, complicated compared to that of PCL-*b*-PB(U) and crystalline homopolymers.

CONCLUSIONS

In this study, the morphology and melting behaviour of the crosslinked PCL-*b*-PB were investigated by WAXS, SAXS, and d.s.c. The WAXD and SAXS results showed that (1) the PCL blocks crystallized in the same crystal form as PCL homopolymers and (2) the microdomain structure in the melt was essentially unchanged on crystallization. These two facts indicated that the PCL blocks crystallized within the fixed microdomain structure to result in the imperfect PCL crystals with a low T_m and a low χ, as examined by d.s.c. measurements. The morphology was, therefore, quite different from that of the uncrosslinked PCL-*b*-PB, where a dramatic morphological reorganization took place by the crystallization. This morphological difference is schematically illustrated in *Figure 10* for the crosslinked and uncrosslinked samples. It is noteworthy that the crosslink introduced in the system changes extremely the morphology after crystallization, so that the crosslink reaction is one of the powerful methods to control the morphology formed in polymer systems containing crystalline chains.

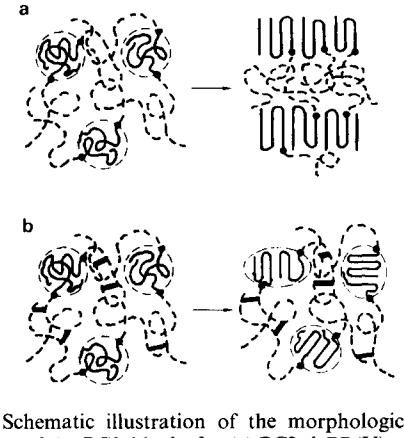

Figure 10 Schematic illustration of the morphological change on crystallization of the PCL blocks for (a) PCL-*b*-PB(U) and (b) PCL-*b*-PB(C). The thick lines connecting broken chains in (b) represent the crosslinks introduced in the system

ACKNOWLEDGEMENTS

This work was supported in part by Grants-in-Aid for Scientific Research (Nos. 07805085 and 08651072) from the Ministry of Education, Science, and Culture of Japan.

REFERENCES

1. DiMarzio, E. A., Guttman, C. M. and Hoffman, J. D., *Macromolecules*, 1980, **13**, 1194.
2. Whitmore, M. D. and Noolandi, J., *Macromolecules*, 1988, **21**, 1482.
3. Unger, R., Beyer, D. and Donth, E., *Polymer*, 1991, **32**, 3305.
4. Nojima, S., Kato, K., Yamamoto, S. and Ashida, T., *Macromolecules*, 1992, **25**, 2237.
5. Rangarajan, P., Register, R. A. and Fetters, L. J., *Macromolecules*, 1993, **26**, 4640.
6. Lovinger, A. J., Han, B. J., Padden, F. J. and Mirau, P. A., *J. Polym. Sci., Part B*, 1993, **31**, 115.
7. Nojima, S., Nakano, H., Takahashi, Y. and Ashida, T., *Polymer*, 1994, **35**, 3479.
8. Ryan, A. J., Hamley, I. W., Bras, W. and Bates, F. S., *Macromolecules*, 1995, **28**, 3860.
9. Nojima, S., Yamamoto, S. and Ashida, T., *Polym. J.*, 1995, **27**, 673.
10. Yang, Y. W., Tanodekaew, S., Mai, S. M., Booth, C., Ryan, A. J., Bras, W. and Viras, K., *Macromolecules*, 1995, **28**, 6029.
11. Cohen, R. E., Cheng, P. L., Douzinas, K., Kofinas, P. and Berney, C. V., *Macromolecules*, 1990, **23**, 324.
12. Veith, C. A., Cohen, R. E. and Argon, A. S., *Polymer*, 1991, **32**, 1545.
13. Ishikawa, S., Ishizu, K. and Fukutomi, T., *Polym. Commun.*, 1991, **32**, 374.
14. Rangarajan, P., Register, R. A., Adamson, D. H., Fetters, L. J., Bras, W., Naylor, S. and Ryan, A. J., *Macromolecules*, 1995, **28**, 1422.
15. Rangarajan, P., Register, R. A., Fetters, L. J., Bras, W., Naylor, S. and Ryan, A. J., *Macromolecules*, 1995, **28**, 4932.
16. Briber, R. M. and Bauer, B. J., *Macromolecules*, 1988, **21**, 3296.
17. Jinnai, H., Hasegawa, H., Hashimoto, T., Briber, R. M. and Han, C. C., *Macromolecules*, 1993, **26**, 182.
18. Sakurai, S., Iwane, K. and Nomura, S., *Macromolecules*, 1993, **26**, 5479.
19. Phillips, P. J. and Kao, Y. H., *Polymer*, 1986, **27**, 1679.
20. Phillips, P. J. and Lambert, W. S., *Macromolecules*, 1990, **23**, 2075.
21. Lambert, W. S., Phillips, P. J. and Lin, J. S., *Polymer*, 1994, **35**, 1809.
22. Shibayama, M., Takahashi, H., Yamaguchi, H., Sakurai, S. and Nomura, S., *Polymer*, 1994, **35**, 2944.
23. Takahashi, H., Shibayama, M., Hashimoto, M. and Nomura, S., *Macromolecules*, 1995, **28**, 5547.

24. Hashimoto, T., Fujimura, M. and Kawai, H., *Macromolecules*, 1980, **13**, 1660.
25. Hashimoto, T., Takenaka, M. and Jinnai, H., *Polym. Commun.*, 1989, **30**, 177.
26. Crescenzi, V., Manzini, G., Calzolari, G. and Borri, C., *Eur. Polym. J.*, 1972, **8**, 449.
27. Chatani, Y., Okita, Y., Tadokoro, H. and Yamashita, Y., *Polym. J.*, 1970, **1**, 555.
28. Wunderlich, B., *Macromolecular Physics 2*. Academic Press, New York, 1976.
29. Rohadi, A., Nojima, S. and Sasaki, S., manuscript in preparation.